

Matthew R. Kramar*
National Weather Service
WFO Amarillo, Texas

and Howard B. Bluestein
Univ. of Oklahoma
Norman, Oklahoma

Andrew L. Pazmany
Univ. of Massachusetts
Amherst, Massachusetts

John D. Tuttle
NCAR
Boulder, Colorado

1. INTRODUCTION

A mobile, non-Doppler 3-cm wavelength radar (Pazmany et al. 2003) was used during the Spring 2001 severe storms season to survey convective storms with a finer spatial and temporal resolution than can routinely be obtained by fixed site radars like the WSR-88D. On several occasions, a hitherto undocumented echo was observed on the radar's reflectivity display, at the back side of developing supercell storms, which we have called the "Owl Horn" signature, owing to the storm's likeness to the profile of the Great Horned Owl. The echo (Fig. 1) is defined by two narrow protrusions in reflectivity at the back side of a developing supercell storm, spanning the entire back edge of the storm, and lasting five to ten minutes before slowly eroding. Since the feature was apparent from various viewing angles with respect to the storm, it was determined that the signature was not an artifact of the radar. The signature was observed on four separate days, on five distinct storms.

In past conference forums, observational results and a wind analysis using the Tracking Radar Echoes by Correlation (TREC) algorithm (Rinehart 1979, Tuttle and Foote 1990) were presented (Kramar et al. 2002), as well as preliminary results of numerical model simulations of storms that produced the "Owl Horn" signature (Kramar et al. 2003). It was seen in the TREC analyses that the reflectivity protrusions were coincident with an arched boundary defined by a wind shift in the storm-relative wind field, which seemed to partition the storm. It was then shown in ARPS model (Xue et al. 1995) numerical simulations (64 km X 64 km X 16 km grid with 1 km horizontal and 500 m vertical resolution) using the ubiquitous Del City composite sounding from 20 May 1977 (e.g. Adlerman et al. 1999) that the coldest (and deepest) air in the storm's outflow (Fig. 2b) was channeled into two narrow protrusions (but still contained in the mass of the cold pool) along the outer edges of the associated cold pool, and that the reflectivity protrusions (Fig. 2a) were collocated with the outflow protrusions. Moreover, elongated bands of upward (downward) vertical velocities (Fig. 2c) were found on the outside (inside) edges of the outflow protrusions with respect to the storm. Most unusual, however, was the presence of elongated banded couplets of vertical vorticity (Fig. 2d) which likewise flanked the outflow protrusions.

Sensitivity tests were conducted to examine the dependence of the "Owl Horn" formation on the hodograph shape and magnitude. It was found that

supercell shear (> 19 m/s, Weisman and Klemp 1982) was a lower-end limit on the necessary shear magnitude, and that hodograph curvature was a requirement on the shape, since no storm generated in a straight-line hodograph environment produced an "Owl Horn" despite producing storm splits like its curved hodograph counterparts.

"Owl Horn" storms, both real and simulated, exhibited storm splits soon after the signature appeared in reflectivity. Model cross sections through the storm confirmed the presence of two distinct precipitation shafts—a structure in agreement with observations—and a pair of midlevel vertical vorticity couplets indicative of splitting supercellular structure. Moreover, it was noted observationally that virtually every storm that exhibited the "Owl Horn" signature (with the only exception being a storm that was rapidly obliterated by a massive outflow boundary soon after exhibiting the signature) went on to produce tornadoes or substantial funnel clouds. It was concluded that the signature forms when small precipitation particles are advected rearward by the low-level banded vorticity couplets, and that it is an indication of an imminent storm split.

Fully explaining the development of the feature, however, requires discovering the source of the vertical vorticity bands that flank the outflow protrusions. To this end, parcel trajectories were calculated, and vorticity computations were made for several parcels in and around the "Owl Horn" signature. The purpose of this paper is to discuss the results of the trajectory/vorticity computations, to examine their implications, and to present recent operational developments in this research.

2. COMPUTATIONS

The vorticity equations in semi-natural coordinates were used, and are given by:

$$\frac{D\omega_s}{Dt} = \omega_n \frac{D\psi}{Dt} + \bar{\omega} \cdot \bar{\nabla} V_H + \frac{\partial B}{\partial n} \quad (1)$$

$$\frac{D\omega_n}{Dt} = -\omega_s \frac{D\psi}{Dt} + \bar{\omega} \cdot \bar{\nabla} (V_H \bar{\nabla} \psi) - \frac{\partial B}{\partial s} \quad (2)$$

$$\frac{D\zeta}{Dt} = \omega_n \cdot \bar{\nabla} w + \zeta \frac{\partial w}{\partial z} \quad (3)$$

where $(\mathbf{s}, \mathbf{n}, \mathbf{k})$ represent orthonormal basis vectors (Lilly, 1982), D/Dt is the derivative following parcel motion, $\bar{\omega}$ is the three-dimensional vorticity vector, vector wind $\vec{V} = (V_H, 0, w)$, ζ is the vertical vorticity, B represents buoyancy, and $\psi = \tan^{-1}(v/u)$. These equations represent the changes in total vorticity in the streamwise (along the flow, Equation 1), crosswise (normal to the flow, Equation 2) and vertical (Equation 3) directions. On the right-hand side of

*Corresponding author address:

Matthew Kramar, 1900 English Road, Amarillo, TX 79108.
Email: matthew.kramar@noaa.gov.

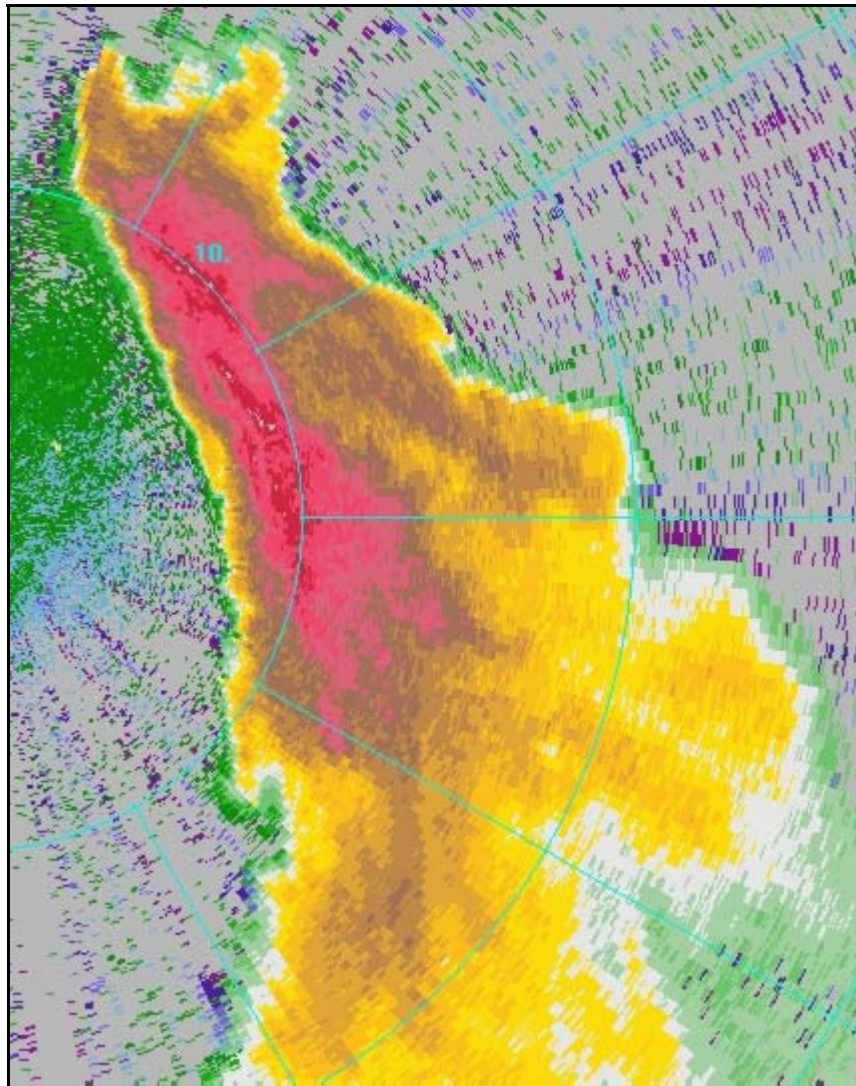


Fig. 1. The “Owl Horn” signature in a low-level PPI on 27 May 2001 near Liberal, Kansas is seen as two reflectivity protrusions at the rear side of the storm (top of image). View is to the north at 1645 CDT. Storm motion is to the southeast. Range rings are at 10 km intervals.

the first two equations, the first terms are interpreted physically as the exchange of streamwise and crosswise vorticity in the plane of motion. The second terms represent the stretching and tilting of streamwise and crosswise vorticity in the plane of motion, and the third terms represent the baroclinic generation of streamwise and crosswise vorticity. In the third equation, the first term on the right-hand side represents the tilting of horizontal vorticity into the vertical, and the second represents the amplification of vertical vorticity by convergence/stretching. The exchange term in the horizontal vorticity equations is relevant primarily in highly curved flows, and so was neglected for purposes of this study based on trajectory results, which showed that

parcel trajectories (those not located in the updraft/downdraft interface) exhibited no significant curvature.

Lines of parcels (at 500 m horizontal parcel spacing and at three vertical levels: $Z = 250$ m, 500 m, and 750 m) were taken through the banded couplets of vertical vorticity. Code from Adlerman et al. (1999) was used (with a three-step Predictor/Corrector and tri-linear interpolation scheme) to compute parcel trajectories 15 min backward and 20 min forward in time from the appearance of the best “Owl Horn” protrusions. For the purposes of this paper, points will be considered at the level of $Z = 750$ m.

The first line of parcels encompassed points located in the region of cyclonic vertical vorticity associated with the

right-flank “Owl Horn” protrusion. Parcels in this line were shown to originate well to the east of the storm, in an environment unaltered by the storm, and were traced generally to a beginning altitude of $Z = 400$ m (Fig. 3, lower right). In forward trajectory calculations, parcels were seen to continue their ascent (up/over the outflow protrusion) while maintaining their westward motion before beginning

a descent on the inside (with respect to the storm) of the outflow protrusion. Parcels from the line traversing the anticyclonic component associated with the right-flank couplet exhibited similar behavior. Backward trajectories showed that the parcels originated east of their present locations, at or around $Z = 300$ m. They were seen to move west, ascend over the outflow protrusion to at or around

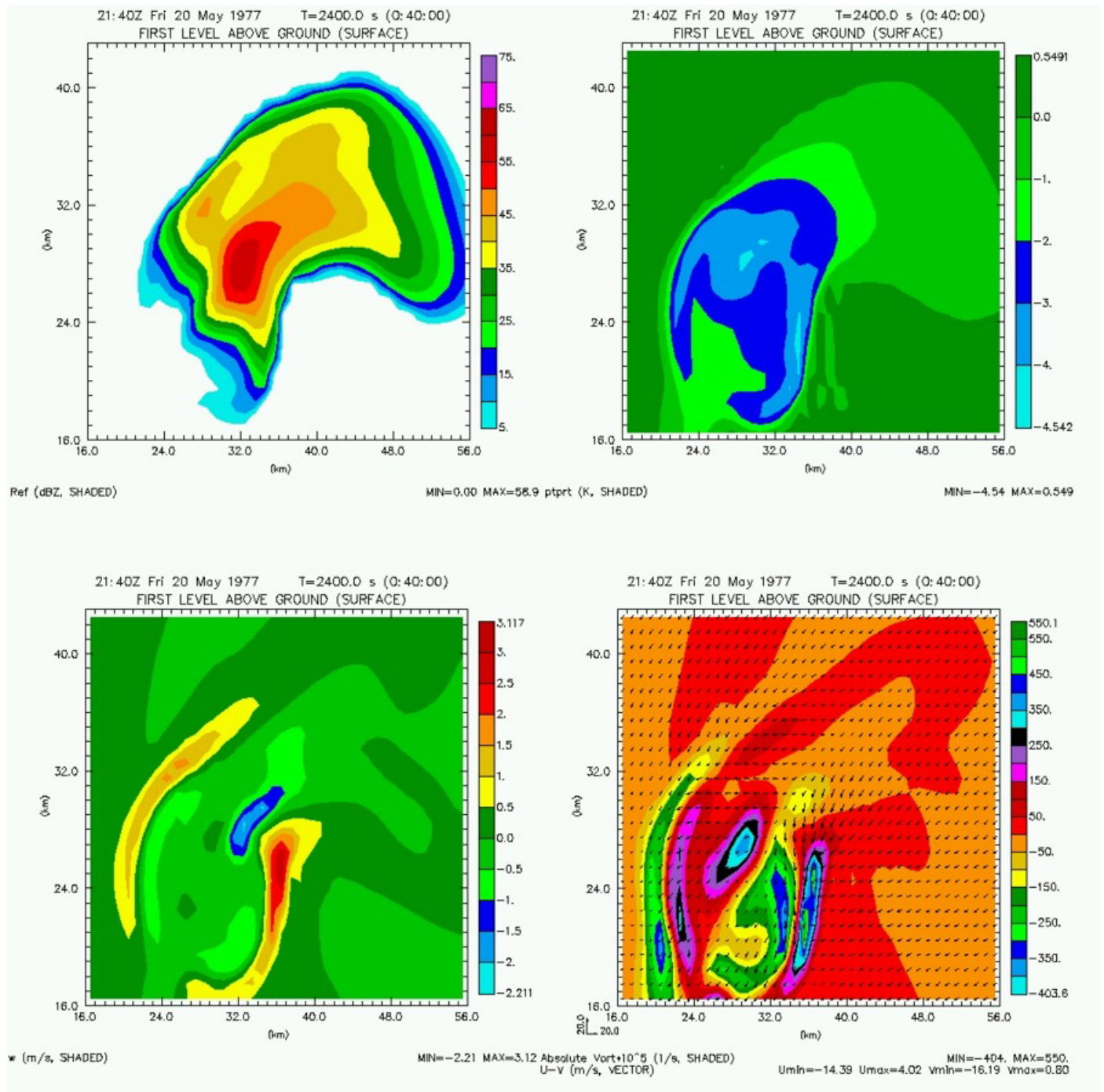


Fig. 2. ARPS model fields at 2140 UTC (2400 s model time) for the control run using the 20 May 1977 Del City composite sounding. Top row from left to right (a) reflectivity, (b) perturbation potential temperature, and bottom row from left to right (c) vertical motion w , (d) vertical vorticity (contours) and storm-relative horizontal wind (vectors).

$Z = 950$ m, and descend to $Z = 750$ m by the time of the reflectivity signature. They were then seen to move generally westward with time in forward trajectory plots.

Similar behavior was noted for parcels associated with the left-flank vertical vorticity couplet. Parcels on both sides of the left-flank outflow protrusion, however, were also shown to originate with a westward component to their motion and outside and to the west of the storm, suggesting that parcels were lifted over the outflow protrusions as the cold pool spread outward and overtook them.

Vorticity analyses were made for points in close proximity to the protrusions in reflectivity. For the point (36 km, 21 km, 750 m) located in the area of cyclonic vertical vorticity associated with the right-flank protrusion, the parcel began with nearly all of its vorticity in the streamwise direction (Fig. 3, upper left). As the parcel moved westward and neared the outflow protrusion, the streamwise vorticity was seen to decrease slowly as the vertical vorticity increased. Since the crosswise vorticity did not cross gradients of vertical motion here, and would only have served to weaken the streamwise vorticity if tilted into the streamwise direction (Fig. 3, upper left), it was primarily the streamwise vorticity that was converted into vertical vorticity as the parcel approached the outflow protrusion. It was seen in a plot of the terms in the vertical vorticity equation (Fig. 3, lower left) that the vertical vorticity of the parcel increased primarily through tilting first, and then through stretching as the parcel was accelerated in the band of upward vertical velocities. Therefore, the cyclonic vertical vorticity component of the right-flank "Owl Horn" was a result of the tilting of streamwise vorticity as the environmental parcels were lifted over the expanding outflow protrusions.

A graph of the terms in the streamwise vorticity equation (Fig. 3, upper right) showed that the parcel's streamwise vorticity had little contribution from horizontal stretching, tilting, or baroclinic generation. Then, since the model was initialized with no vorticity beyond the ambient, and parcels in the source region did not acquire streamwise vorticity through tilting, stretching or baroclinic generation, the vorticity must have been acquired initially from the environmental wind shear (although as the parcel interacts with the boundary, it is not unreasonable to expect the parcel to increase its vorticity through baroclinic generation, as seen in the graph).

A parcel located in the anticyclonic component of the right-flank "Owl Horn," (32.5 km, 20.5 km, 750 m), was seen (not shown) to originate on the cyclonic side of the outflow protrusion: initially the parcel exhibited cyclonic vertical vorticity, but the tilting term began to act less as the parcel reached the apex of its trajectory; as the parcel was influenced by the downward vertical velocities on the inside of the outflow protrusion, tilting began to decrease positive vertical vorticity, allowing the parcel to acquire anticyclonic vertical vorticity, which was similarly stretched.

The same process was effected in reverse for the left-flank vertical vorticity couplet. Since parcel motion was away from the expanding outflow, streamwise vorticity

was oriented to the west along the parcel motion. When the parcels encountered the upward vertical velocities at the leading edge of the outflow protrusion, the sense of the horizontal vorticity became tilted with a downward orientation, increasing the vertical vorticity negatively. As the parcels began to descend on the inside of the outflow protrusion, the sense of the vorticity was reversed through tilting. Further detailed analysis of the left-flank couplet will be omitted herein to avoid repetition and conserve space, but will be included in the conference presentation.

3. SUMMARY AND CONCLUSIONS

The "Owl Horn" signature formation is dependent upon the development of elongated bands of vertical vorticity in the low levels that flank elongated protrusions in the storm outflow. But a vorticity analysis has shown that the vorticity couplets are dependent on the development of the outflow protrusions. So the process is a positive feedback mechanism: streamwise vorticity (environmental and baroclinically generated) is tilted into the vertical by the expanding outflow protrusions, which in turn advects and elongates the outflow protrusions further rearward.

A conceptual model of the process by which the vorticity couplets are generated is given in Fig. 4. It is apparent from this figure that the initial configuration of the outflow is responsible for the entire process. If the deepest (and coldest) outflow is not initially at the periphery of the cold pool, then a supercritical head [akin to that seen in two-dimensional simulations of Xu (1992)] will not form, and rather, the cold pool will spread out more uniformly as is seen in the straight line hodograph simulations. Also highly relevant, however, is the hodograph curvature, since it could help induce a supercritical head in the outflow by a damming effect through opposition to its motion by the low-level winds, but more importantly, it reorients the horizontal vorticity vector from a direction parallel to the outflow boundary motion to one with a component across the boundary—thus allowing for tilting of horizontal vorticity to take place.

By way of numerical simulations, the process through which the "Owl Horn" signature develops has been identified, and its dependence on the environmental wind shear was examined. Every storm, both real and simulated, that produced an "Owl Horn" signature exhibited several signs of a forthcoming split concurrent with the appearance of the feature: a second precipitation shaft developing on the left side of the storm with respect to its motion in both observed and simulated storms; a second vorticity couplet in the mid-level simulated wind field; and a second maximum in reflectivity on the left side of the simulated storm with respect to its motion which becomes more separated with height. Soon after the "Owl Horn" appears, the storm split comes to fruition in both observed and simulated cases. While not every splitting storm exhibits an "Owl Horn" signature, every storm that exhibited the echo underwent a splitting process soon after. Based on this study, it is suggested that the "Owl Horn" signature in reflectivity is an indication of a strengthening supercell and an imminent storm split.

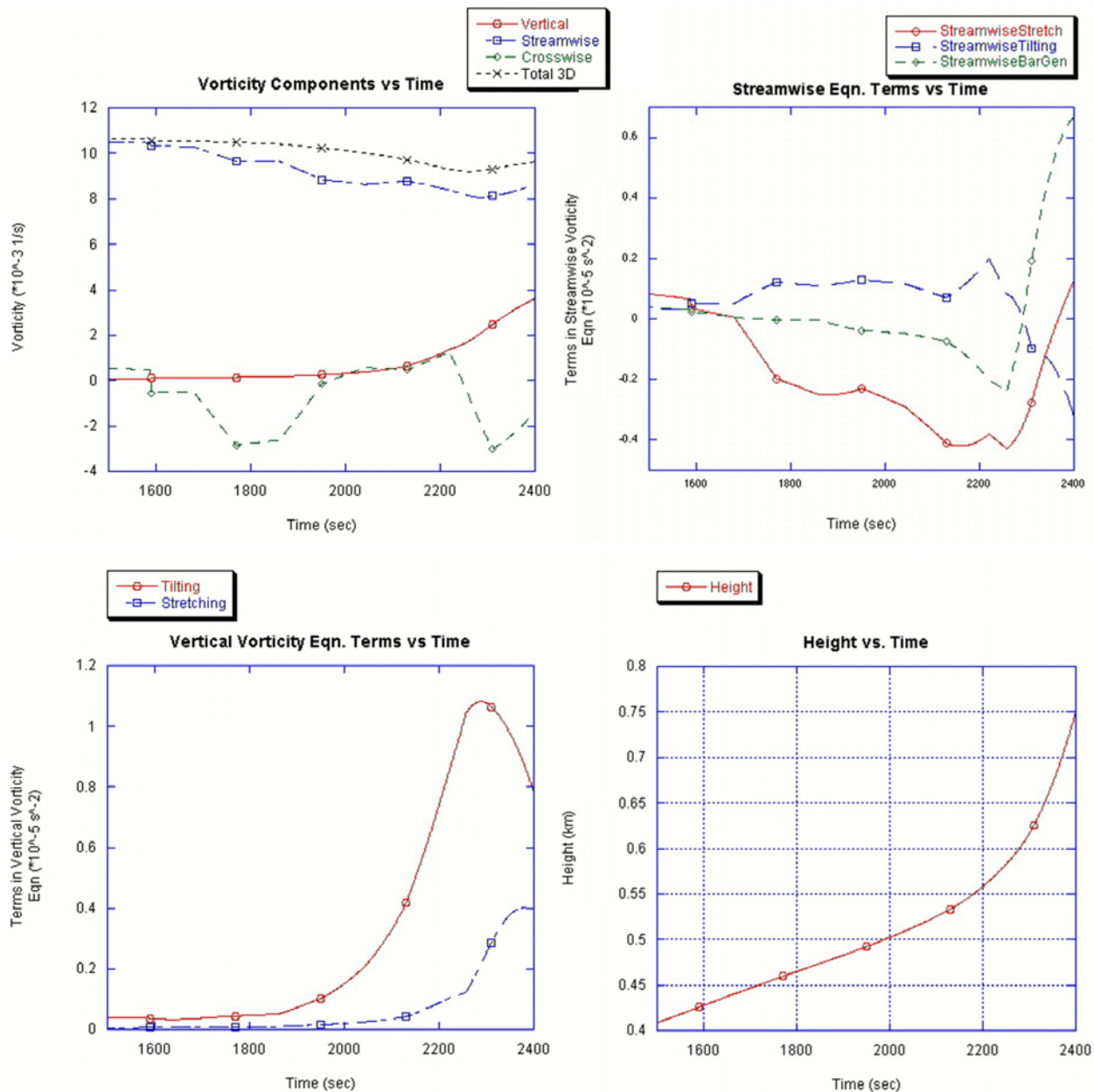


Fig. 3. For parcel (36 km, 21 km, 750 m) located in the cyclonic vortex associated with the right-flank “Owl Horn” at 2140 UTC (2400 s model time), four-panel plot of (upper left) parcel’s total vorticity and components of total vorticity; (upper right) terms in the streamwise vorticity equation; (lower left) terms in the vertical vorticity equation; (lower right) plot of parcel height versus time for the parcel being examined.

Several “Owl Horn” echoes were observed with the UMass radar during the 2004 storm season, including storms on 12 May and 29 May. In addition, the signature was observed with the SMART-Radar (Biggerstaff and Guynes 2000) on 15 May 2003 in a storm near Lela, Texas. But of primary interest was the documentation of two instances of the signature on the WSR-88D radar at Amarillo, Texas. The feature was observed on 17 June and 21 June 2004 in close proximity to the radar. It was

hitherto thought that the WSR-88D network would be incapable of resolving the “Owl Horn” signature owing to its temporal scanning pattern of the low levels of the atmosphere (where the signature is apparent) and its spatial resolution. But in light of these recent observations, the forecasting utility of the signature presents itself, since it can alert operational forecasters to the intensity of a storm (in some instances, well ahead of time—in the case of WFO Amarillo, a full 45 minutes before baseball-size hail

ravaged western Amarillo, and almost 20 minutes before the first of seven tornadoes was reported on 21 June). In all of these cases, storms were observed to split soon after the signature appeared, and all went on to produce documented tornadoes. Although no evidence beyond the observational has yet been established, perhaps there is an association between "Owl Horn" production and greater likelihood of tornadic circulations developing in the storm at a later time owing to enhanced low-level cyclonic vertical vorticity generation along the right-flank gust front.

4. ACKNOWLEDGMENTS

This research was funded by NSF grant ATM-9912097 at the University of Oklahoma (OU) and ATM-0000592 at UMASS. Support was provided by Mark Laufersweiler and staff, and the School of Meteorology at OU. Edwin Adlerman, Ming Xue, Christopher Weiss, Allison Silveira, Alan Shapiro, Frederick Carr, and Donald Burgess provided invaluable help and advice. Technical assistance was provided by Jason Jordan and Richard Wynne at WFO Amarillo. NCAR is supported by the National Science Foundation. Simulations were run by computers at the Center for Analysis and Prediction of Storms (CAPS) at OU.

5. REFERENCES

- Adlerman, E.J., K.K. Droegemeier and R. Davies-Jones, 1999: A numerical simulation of cyclic mesocyclogenesis. *J. Atmos. Sci.* **56**, 2045-2069.
- Biggerstaff, M.I., and J. Guynes, 2000: A new tool for atmospheric research. *Preprints, 20th Conf. Severe Local Storms*. Orlando, FL, Amer. Met. Soc., 277-280.
- Kramar, M.R., H.B. Bluestein, A.L. Pazmany, and J.D. Tuttle, 2002: The "Owl Horn" radar signature in developing supercells. *Preprints, 21st Conf. Severe Local Storms*. San Antonio, TX, Amer. Met. Soc., 210-213.
- Kramar, M.R., H.B. Bluestein, A.L. Pazmany, and J.D. Tuttle, 2003: The "Owl Horn" radar signature in developing Southern Plains thunderstorms. *Preprints, 31st Conf. Radar Meteorology*. Seattle, WA, Amer. Met. Soc., 567-570.
- Lilly, D.K., 1982: The development and maintenance of rotation in convective storms. *Intense Atmospheric Vortices*, L. Bengtsson and J. Lighthill, Eds., Springer-Verlag, 149-160.
- Pazmany, A.L., F.J. Lopez, H.B. Bluestein, and M.R. Kramar, 2003: Quantitative rain measurements with a mobile, X-band, polarimetric Doppler radar. *Preprints, 31st Conf. Radar Meteorology*. Seattle, WA, Amer. Met. Soc., 858-859.
- Rinehart, R.E., 1979: Internal storm motions from a single non-Doppler weather radar. NCAR/TN-146+STR, 262pp.
- Tuttle, J. D., and G. B. Foote, 1990: Determination of the single boundary layer airflow from a single Doppler radar. *J. Atmos. Oceanic Technol.*, **7**, 218-232.
- Xu, Q., 1992: Density currents in shear flows—A two-fluid model. *J. Atmos. Sci.*, **49**, 511-524.
- Xue, M, K.K Droegemeier, V. Wong, A. Shapiro, and K. Brewster, 1995: *ARPS Version 4.0 User's Guide*. Center for Analysis and Prediction of Storms, University of Oklahoma, 380pp.

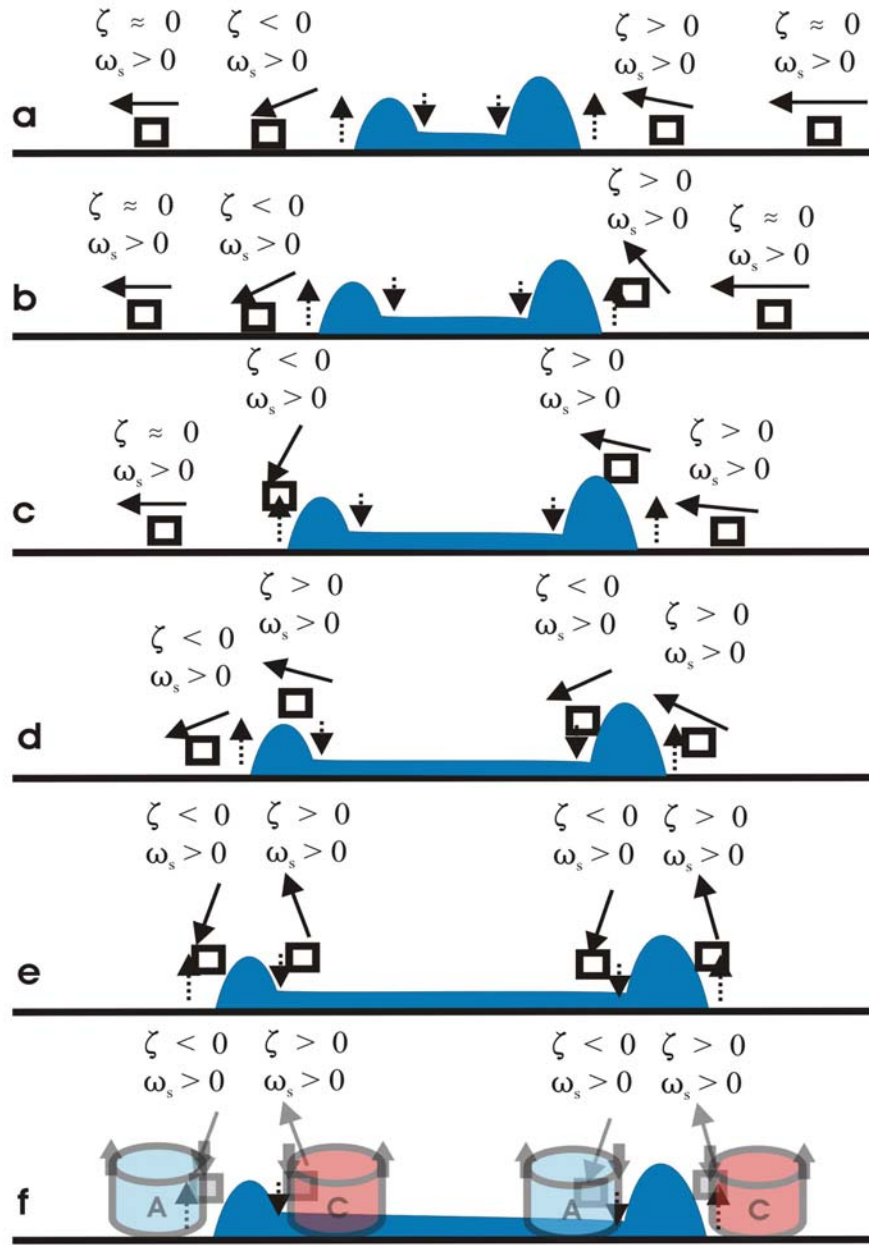


Fig. 4. A conceptual model in the X-Z plane to explain how the vorticity couples are generated by weak protrusions in the outflow. (a) Outflow initially moves outward, with weak upward motion along the outer edges and weak downward motion on the inside. Parcels are initially moving in the sense of the vorticity vectors (arrows) since nearly their entire vorticity is focused in the streamwise direction. (b) As parcels approach the oncoming outflow, they encounter a gradient of vertical motion, which tilts the horizontal component of their streamwise vorticity vertically. Stretching also acts on the tilted vorticity to enhance it. (c) As parcels reach the peak of the outflow protrusions, their motion levels out and the vertical vorticity weakens as tilting begins acting to generate less positive vertical vorticity. (d) As parcels begin their descent, they encounter a gradient of downward motion, which tilts their horizontal vorticity into the vertical again, but in the opposite direction. Thus the vertical vorticity changes sign. (e) The process continues as the outflow expands further. (f) Vertical vorticity couples [cyclonic (C) and anticyclonic (A)] are generated and work in tandem to advect the cold protrusions further rearward, creating the “Owl Horn” signature in the outflow field. Smaller precipitation particles from the downdraft are similarly advected by the vortices, creating the protrusions in storm reflectivity.